Evaluation of the ability of an artificial neural network model to simulate the input-output responses of a large karstic aquifer: the La Rochefoucauld aquifer (Charente, France)

Bedri Kurtulus · Moumtaz Razack

Abstract The ability of artificial neural networks (ANN) to model the rainfall-discharge relationships of karstic aquifers has been studied in the La Rochefoucauld karst system, south-west France, which supplies water to the city of Angoulême. A neural networks model was developed based on MLP (multi-layer perceptron) networks and the Levenberg-Marquardt optimization algorithm. Raw rainfall data were used without transformation into effective rainfall. This allowed for the elimination of certain non-verifiable simplifying assumptions and their subsequent introduction into the modeling procedure. The raw rainfall and discharge data were divided into three groups for the training, the validation and the prediction test of the ANN model. The training and validation phases led to a very satisfactory calibration of the ANN model. The attempt to predict discharges showed that the ANN model is able to simulate the karstic aquifer discharges. The shape of the simulated hydrographs was found to be similar to that of the actual hydrographs. These encouraging results make it possible to consider interesting and new prospects for the modeling of karstic aquifers, which are highly non-linear systems.

Résumé L'aptitude des réseaux de neurones artificiels (RNA) à modéliser les relations pluie-débit des aquifères karstiques a été évaluée sur le karst de La Rochefoucauld (Sud-Ouest de la France), qui fournit l'eau potable à la capitale régionale Angoulême. Un modèle RNA a été développé à cet effet, basé sur les réseaux PMC (Perceptron Multicouche) et l'algorithme d'optimisation de Levenberg-Marquardt. Les données de pluie utilisées concernent la pluie brute, sans transformation en pluie efficace, ce qui permet de s'affranchir de certaines hypothèses simplificatrices non vérifiables. Les données de pluie brute et de débit ont été réparties en 3 groupes pour l'apprentissage, la validation et le test de prédiction du RNA. Les phases d'apprentissage et de validation ont permis d'aboutir à une calibration très satisfaisante du modèle RNA. La tentative de prédiction a montré que le RNA est apte à simuler les débits de l'aquifère karstique à partir de la pluie brute. La forme des hydrogrammes simulés est semblable à celle des hydrogrammes réels. Les résultats obtenus sont très encourageants et permettent d'envisager des perspectives intéressantes et nouvelles de modélisation des aquifères karstiques, qui sont des systèmes hautement non-linéaires.

Resumen Se ha estudiado la capacidad de las redes artificiales neurales (ANN) para modelizar las relaciones de lluvia-descarga de acuíferos kársticos en el sistema kárstico La Rochefocauld, al suroeste de Francia, el cual abastece de agua a la ciudad de Angoulême. Se desarrolló un modelo de redes neurales en base a redes MLP (Perceptron Multi-Capas) y el algoritmo de optimización Levenberg-Marquardt. Se utilizaron datos de lluvia sin la transformación hacia lluvia efectiva. Esto permitió la eliminación de ciertos supuestos simplificadores no verificables y su subsiguiente introducción en el procedimiento de modelizado. Los datos brutos de descarga y lluvia se dividieron en 3 grupos para la preparación, validación y la prueba de predicción del modelo ANN. Las fases de preparación y validación llevaron a una calibración muy satisfactoria del modelo ANN. El intento por predecir descargas mostró que el modelo ANN es capaz de simular las descargas del acuífero kárstico. Se encontró que la forma de los hidrogramas sintéticos es similar a la de los hidrogramas reales. Estos resultados alentadores hacen posible considerar prospectos nuevos e interesantes para el modelizado de acuíferos kársticos los cuales son sistemas altamente no-lineares.

Keywords Artificial neural networks · Karst · Numerical modeling · Non-linear system · La Rochefoucauld aquifer

Received: 26 September 2005 / Accepted: 13 June 2006
Published online: 23 September 2006

B. Kurtulus · M. Razack (✉)
Hydrogeology Department (UMR6532),
University of Poitiers,
40 avenue du Recteur Pineau, Poitiers, Cedex 86022, France
e-mail: moumtaz.razack@univ-poitiers.fr

Introduction

Karstic aquifers are largely widespread on a worldwide scale since 12% of the emerged grounds are represented by carbonated rocks, and they contain significant water resources. Almost one quarter of the world population relies on groundwater from karst systems (Ford and William 1989). In France, drinking water in several large cities (Montpellier, Angoulême, etc.) is supplied by this type of aquifer. Like any other groundwater resource, karstic aquifers must necessarily be exploited within the framework of a sustainable management strategy. To this end, numerical models are efficient and relevant tools, especially for predicting aquifer responses to climatic changes, which are nowadays evolving towards drought.

Karstic aquifers are strongly heterogeneous and discontinuous systems whose hydrodynamic functioning can be highly complex. They are dominated by secondary (fracture) and tertiary (conduits) porosities. The conceptual models of these aquifers are represented by the juxtaposition of highly transmissive conduits and discontinuities together with fractured blocks of low transmissivity (Kiraly 1975; Drogue 1992; Padilla and Pulido-Bosch 1995; Amraoui et al. 2003; Rahnemai et al. 2005). Following heavy rainfall, quick and probably turbulent flow first occurs within the transmissive conduits which make up the karstic network. Spring discharges from these systems can also reach several (even several tens) m^3/s in flood periods. By contrast, in periods of depletion, flow in the karstic network can become negligible. These systems are thus very organized and exhibit hierarchical flow paths (Mangin 1984).

Distributed numerical groundwater models have been successfully developed for aquifers with interstitial porosity, since the continuity of these aquifers is unquestionable. In addition, these numerical models are based on Darcy's law and assume laminar flow, so they are well adapted to interstitial porosity aquifers. Their application to karstic aquifers is, however, quite problematical, even unrealistic, at least on local or intermediate scales (Huntoon 1995; Scanlon et al. 2003). Attempts to model karst aquifers using spatially distributed numerical models proved successful on a regional scale for management purposes (Angelini and Dragoni 1997; Larocque et al. 1999). Unfortunately, this type of numerical model requires quite large databases (permeability, porosity, transmissivity, piezometry, etc.), specifically when the system is heterogeneous, as are karst aquifers.

However, modeling remains an important and essential predictive tool for the management of aquifer water resources. In this context, the objective of this work is to evaluate the ability of the modeling method known as ANN (artificial neural networks) to simulate groundwater flow in karstic aquifers. Artificial neural networks (ANN) are at present largely accepted in the scientific literature for the modeling of nonlinear and dynamic systems. They are particularly useful in situations where the physical processes governing input–output responses are not entirely understood.

Over the last decade, the ANN method has been considerably developed in surface hydrology. Various authors have shown the ability of ANN to forecast surface flows (French et al. 1992; Halff et al. 1993; Hsu et al. 1995; Shamseldin 1997; Minns and Hall 1996; Sajikumar and Thandaveswara 1999; Imrie et al. 2000; Rajurkar et al. 2004). By comparison, applications in hydrogeology are more recent and relatively few. Zio (1997) examined the ability of ANN to solve the inverse problem in hydrogeology. Aziz and Wong (1992) and Balkhair (2002) used ANN to estimate aquifer parameters. Several authors used ANN to assess groundwater quality (Kuo et al. 2004) or to solve groundwater remediation issues (Ranjithan et al. 1993; Rogers et al. 1995). Morshed and Kaluarachchi (1998) performed a very informative study on the efficiency of ANN in flow and transport simulations in porous media. Lallahem and Mania (2003) used ANN to simulate fractured porous media.

The use of ANN for simulating karst aquifers is, however, uncommon. The karstic aquifer taken as example in this study is the La Rochefoucauld aquifer located in the Charente Region, western France (Larocque and Razack 1998). This aquifer is very important to the regional economy as it provides drinking water to the regional capital, the city of Angoulême. The discharge rate of the main outlet of the aquifer, the La Touvre spring, which is the second most important spring in France after the Fontaine de Vaucluse (in southern France), can vary between 2 and 40 m^3/s.

The ANN (artificial neural networks) approach

This paper provides an overview of the ANN theory. Interested readers can find in-depth descriptions of the ANN theory in several references (Fausett 1994; Beale and Jackson 1991; Maren et al. 1990). The ANN, as indicated by the term, is based on the understanding of the problem solving process of the human brain. The structure of an ANN works like the human brain, which applies knowledge gained from experience to solve new problems. Accordingly, the ANN can be used in powerful computations of complex nonlinear relationships. A neural network can be viewed as a nonlinear input–output model. In the present work, it will be used to model the raw daily rainfall-discharge process in a karst aquifer (i.e. using rainfall data without transformation into effective rainfall).

A neural network is made up of a number of nodes, which are the processing elements of the network and are usually called ‘neurons’. Each neuron is connected to other neurons, receives an input signal, processes it and transforms it into an output signal. The input signal can be single or an array of signals, whereas the output signal is always single. The kind of network used in this study is a multi-layer feedforward neural network, in which the neurons are arranged in layers (Fig. 1). A layer is a group of neurons having the same pattern of connection with the neurons in the other layer(s). The multi-layer feedforward neural network comprises an input layer, an output layer and one or more layers in between called hidden layers. Figure 1 shows a typical three-layer feedforward network. As shown in this figure, in a feedforward neural network, information moves in one direction only.

Each layer plays a different role in the overall operation of the network. The input layer receives an external input

 DOI 10.1007/s10040-006-0077-5

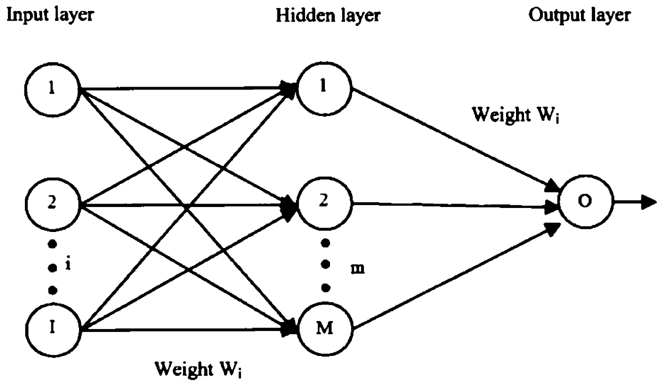

Fig. 1 General architecture of a multi-layer feedforward artificial neural network. *I* final number of neurons (*i*) in the input layer; *M* final number of neurons (*m*) in the hidden layer

array (input data). Each input neuron receives a single element of this array and relays that element to all the neurons of the next layer (i.e. the hidden layer in the three-layer feedforward network). The hidden layer has no connecting path to external inputs or outputs. This layer reinforces the ability of the network to process robustly and efficiently complex nonlinear systems (Medsker 1994). In the three-layer feedforward network, each hidden neuron receives an input array from the input layer. It transforms this input array into a single output that is transferred to the output layer. In turn, each output neuron transforms the inputs received from the hidden layer into an output. All the outputs of this layer constitute the response of the network to the external inputs.

In the hidden and output layers, the input Yi to a neuron i has the following general formula:

$$Y_i = \sum_{j=1}^{n} W_{ji} X_j + \theta_i \tag{1}$$

where W_{ji} is the weight vector of neuron i; n is the number of neurons in the layer preceding the one containing the neuron i; X_j is the output from neuron j; θ_i is the neuron threshold value, which constitutes a means to scale Eq. (1) into a useful range and consequently enhance the network flexibility (Maren 1990; Shamseldin 1997).

The weighted sum (1) is afterwards transformed into the output Z_i from neuron i through a nonlinear transfer function f. The transfer function is usually a non-linear, smooth and monotonically increasing function. Several types of transfer functions are available. The same transfer function is generally used for all neurons in the hidden and output layers. The transfer function must be differentiable for optimization purposes. The transfer function used in this study is the sigmoid function which has the following expression:

$$Zi = 1./(1 + exp(-Yi)) \tag{2}$$

The sigmoid transfer function allows non-linearity to be introduced in the neural network processing and is broadly used in ANN modeling (Shamseldin 1997). Multi-layer feedforward neural networks are also referred to as multi-layer perceptrons (MLP).

In practical applications, the number of neurons in the input and output layers is determined by the data to be processed by the network. Each element of the external input array is assigned to one neuron of the input layer. There are as many neurons in the output layer as there are elements in the external output array. The number of hidden layers should not be large, in order not to slow the network efficiency. One hidden layer is generally recommended in the literature (Masters 1993). The number of neurons in the hidden layer is arbitrary and should be neither too small nor too high. Too few neurons may deteriorate the network performance, whereas too many neurons may lead to over-fitting (over-training) the network without actually improving its performance. Generally, a trial and error procedure is carried out to select the appropriate number of hidden neurons.

Once the structure of the ANN has been selected, the next phase is the training of the network. The training process consists of determining the ANN weights and biases. This procedure is similar to the calibration procedure in hydrogeological modeling. The purpose is to make sure that the network actually extracts the required features from the data sets. The ANN is trained with a set of input and known output data. The goal is to determine a set of connection weights so that the ANN simulates output values as close as possible to the known output values. When the difference between known and estimated values is less than a specified value, the ANN is considered trained.

The backward-error propagation training algorithm is commonly used for the training of multi-layer feedforward ANN (Hagan et al. 1996). Because of this popularity, multi-layer perceptrons are often referred to as back-propagation neural networks. The backpropagation algorithm uses a set of input and known output data. The input data set is used by the ANN to estimate an output array, which is then compared with the known output array. As stated above, when the difference is less than a specified value, training is stopped. By contrast, if the difference is significant, the weights are changed while moving backwards through the network to reduce the difference. The neural network training is performed using a backpropagation algorithm. Various numerical optimization methods are available for the ANN training. In this work, the Levenberg-Marquard algorithm was used (Moré 1978; Press et al. 1992). This algorithm trains neural networks at a rate 10 to 100 times faster than the usual gradient descent back-propagation method (Hagan and Menhaj 1994). The ANN model was developed using the Neural Networks Toolbox of the MATLAB software (Demuth and Beale 2003).

For practical purposes, performing a modeling task using ANN comprises three phases, which are the training, validation and testing (or prediction) phases of the network. During the training phase, the difference between known and estimated values decreases, tending asymptotically towards zero. The ANN learns more and more about the

 DOI 10.1007/s10040-006-0077-5

data which are presented to it. However, a continued training would result in overfitting of the training data and the ANN's generalization ability would not be operational. Generalization ability is defined as a network's ability to perform well on data that were not used to calibrate it (Cheng and Titterington 1994). The goal of the validation phase is then to stop the training early if the performance of the network on the validation arrays does not improve. The training is stopped when the validation error is observed to bottom out and start increasing. The validation phase prevents over-training of the network, i.e. it prevents the network from learning the noise present in the data. After the training and validation have been completed, the ANN is considered calibrated (i.e. all the connection weights are determined) and ready to be used for forecasting purposes. However, before using the ANN to forecast unknown outputs, its actual predictive performance must be tested by comparing outputs estimated by the calibrated ANN with known outputs. At each phase (training, validation and prediction), the ANN performance is measured by the determination coefficient of goodness-of-fit R^2:

$$\mathrm{R}^2 = 1 - \frac{\mathrm{V_R}}{\mathrm{V_T}} \tag{3}$$

where V_{T} is the total variance of the known output vector and V_{R} is the residual model variance. Let Q_{i} be the output variable, then the total variance and the residual variance are expressed as:

$$V_{\mathrm{T}} = \frac{1}{N}\sum\left(Q_{\mathrm{i}} - \overline{Q}\right)^2 \tag{4}$$

$$V_{\mathrm{R}} = \frac{1}{N}\sum\left(Q_{\mathrm{i}} - \widehat{Q}_{\mathrm{i}}\right)^2 \tag{5}$$

where Q_{i} is the observed value; $\overline{Q}$ is the arithmetic mean; $\widehat{Q}_i$ is the ANN model estimated value.

For the prediction phase, three more criteria are used: the mean residual error (ME), the mean absolute residual error (MAE) and the root mean square error (RMSE). They are given by:

$$\mathrm{ME} = \frac{1}{N}\sum\left(\widehat{Q}_{\mathrm{i}} - Q_{\mathrm{i}}\right)^2 \tag{6}$$

$$MAE = \frac{1}{N}\sum\left|\left(\widehat{Q}_{\mathrm{i}} - Q_{\mathrm{i}}\right)\right| \tag{7}$$

$$RMSE = \left[\frac{1}{N}\sum\left(\widehat{Q}_{\mathrm{i}} - Q_{\mathrm{i}}\right)^2\right]^{1/2} \tag{8}$$

The La Rochefoucauld karstic system

The La Rochefoucauld karstic aquifer is located in Middle and Upper Jurassic limestones, close to the city of Angoulême (Charente, France; Fig. 2). The whole aquifer lies on the impermeable Aalenian-Toarcian marls. It is closed to the west by a quasi-impermeable limit formed of a thick series of marls and marly limestones along the Fault of Echelle. To the west, the Kimmeridgian marls and marly limestones constitute a cover of the aquifer of very low permeability. The total thickness of the Middle and Upper Jurassic limestones (Fig. 3) ranges from 0 m where the Aalenian outcrops, to 550 m on the western limit. Their karstification dates from the emergence of the area during the Lower Cretaceous (Rouiller 1987). Diving explorations (Rambaud 1979) showed that the principal conduit uplifting water to the outlets goes down beyond 130 m in depth. Drillings located downstream on the karst showed very deep water flows. These observations indicate that the karstified and transmissive zone is very thick. The aquifer is free over its almost total extent and covers an area of 600 km^2.

The aquifer possesses two discharge systems known as the La Touvre and La Lèche springs. The waters of the La Touvre spring, of very good quality, are collected by the town of Angoulême as a drinking water supply. The La Lèche spring is intermittent and constitutes a secondary discharge system of the aquifer, located approximately 500 m from the La Touvre spring. The discharge rates of the La Touvre spring vary between 2 and 40 m^3/s.

Four rivers flow over the La Rochefoucauld karst. The Bandiat and the Tardoire rivers have their source in the Massif Central. They are not perennial and undergo significant losses when they enter in contact with karstified limestones. Together, the Bandiat and the Tardoire rivers account for more than 50% of the outlet discharges. The Bonnieure River, which flows in the northern sector of the aquifer, is perennial. The Echelle River flows in the south-west of the aquifer.

Several tracer tests were carried out, with dye tracers injected in sinkholes ('Chez Lacoux', 'Puy Vidal', 'Champ de la Queue', 'La Boissière', 'Guillot'; Fig. 2) located in the northern sector of the aquifer (Quélennec et al. 1971). The results show transport velocities and dispersivities, ranging from 40 to 100 m/h and from 10 to 200 m, respectively (Larocque and Razack 1998). Velocity values are high and dispersivity values are relatively low compared to other karst systems (Barrett and Charbeneau 1996; Ross et al. 2001). These results show that transport is primarily convective, rapid, with a weak spreading out of the tracer cloud. Such transport properties are characteristic of a well-karstified medium.

There is a great number of wells exploiting the La Rochefoucauld aquifer. Pumping tests were carried out on these supply wells, but no observation wells were available. Only about 15 tests could be reinterpreted by the method of

 DOI 10.1007/s10040-006-0077-5

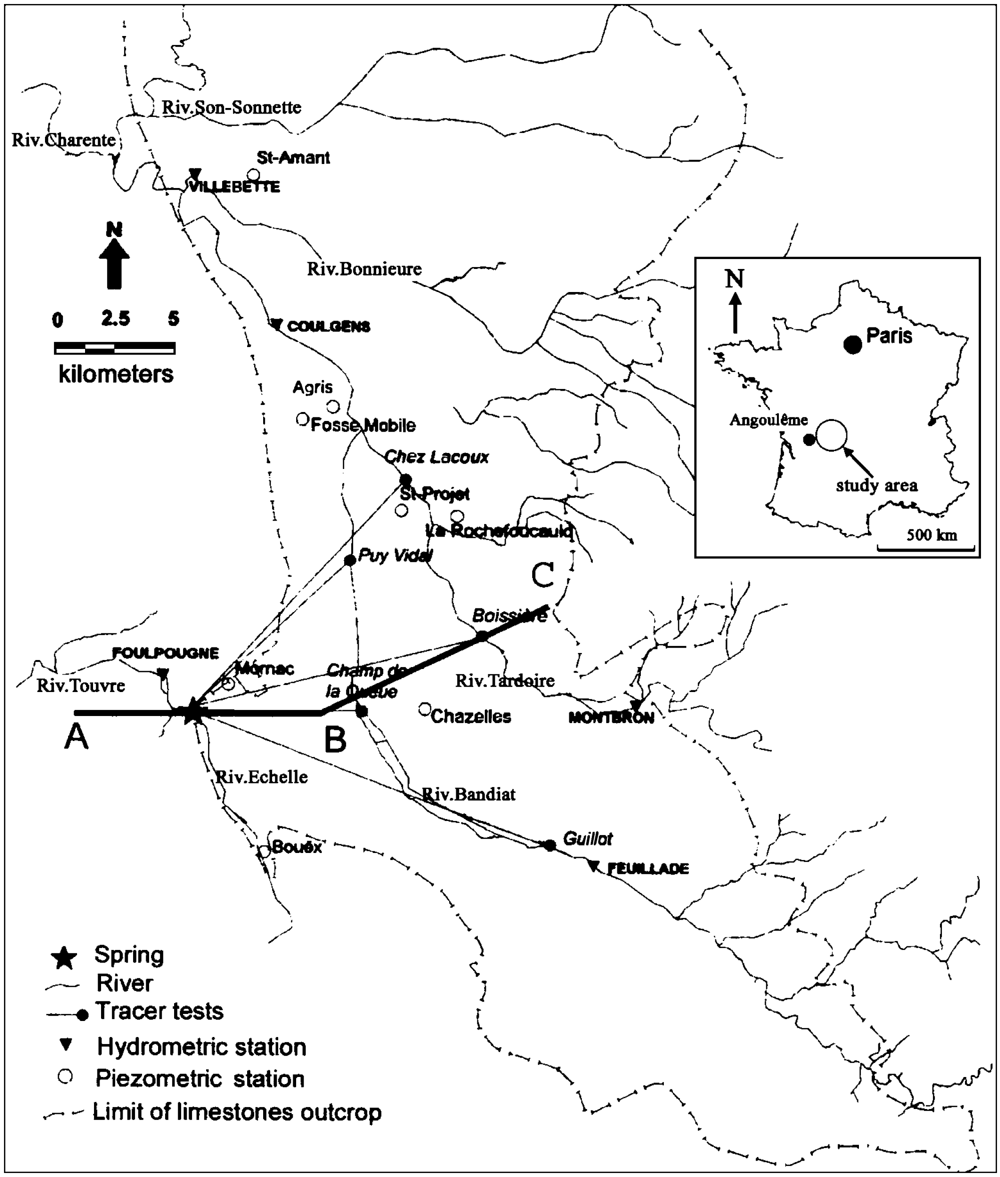

Fig. 2 **a** France, and **b** The La Rochefoucauld karst system

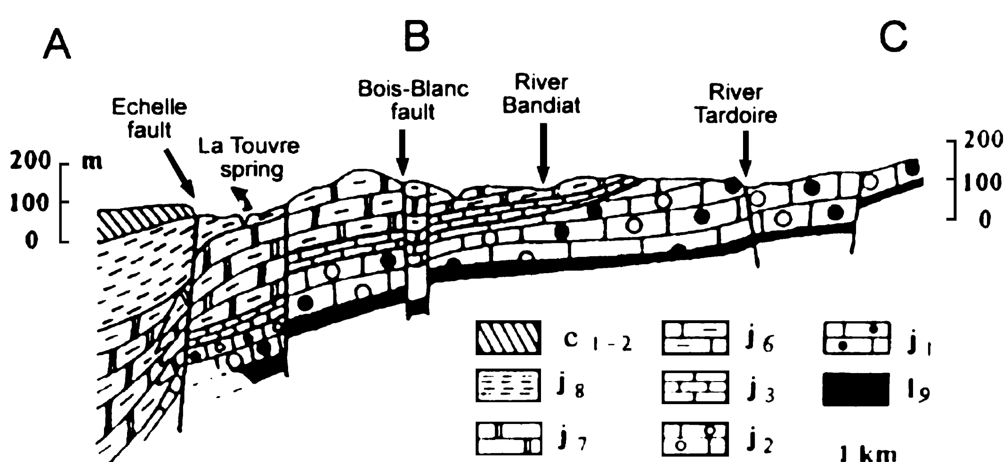

Fig. 3 Cross section of the La Rochefoucauld karst system. $c_{1–2}$ Cenomanian; $j_{7–8}$ Kimmeridgian; j_6 Oxfordian; j_3 Callovian; j_2 Bathonian; j_1 Bajocian; l_9 Toarcian-Aalenian

 DOI 10.1007/s10040-006-0077-5

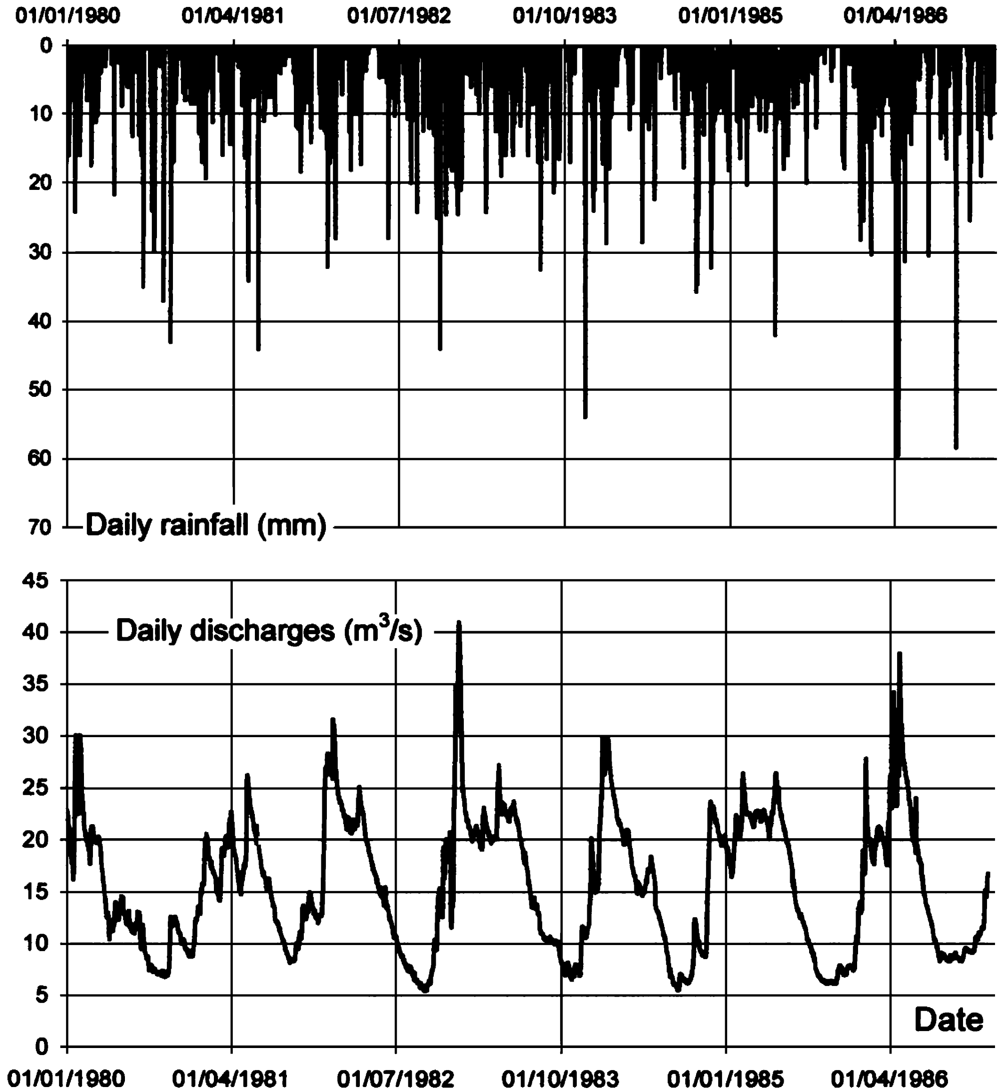

Fig. 4 Daily rainfall and discharges data over 7 years (1 January 1980–31 December 1986)

Jacob (Kruseman and de Ridder 1994). This method assumes that the pumping-induced flow is of Darcian type and is comparable to that of an equivalent porous medium. Whenever the method of Jacob was not applicable, the pumping tests were not interpreted because of the lack of information about the tested medium structure. The transmissivity values calculated using the few interpretable tests are, however, very variable in space. The transmissivity values vary between 2.10^{-4} and 4.10^{-2} m^2/s. They thus spread over three orders of magnitude and clearly point out the strong heterogeneity of the aquifer (Larocque and Razack 1998).

A network of hydrometric stations has been set up on the La Rochefoucauld karst (Fig. 2). The data used in this study are daily data and come from the La Rochefoucauld station for the rainfall and from the Foulpougne station for the discharges. The Foulpougne gaging station is located downstream of the outlets of the karstic aquifer and thus takes into account the discharges of all outlets, La Touvre and La Lèche. The rainfall-runoff data used here span the period between January 1, 1980 and December 31, 1986 (Fig. 4).

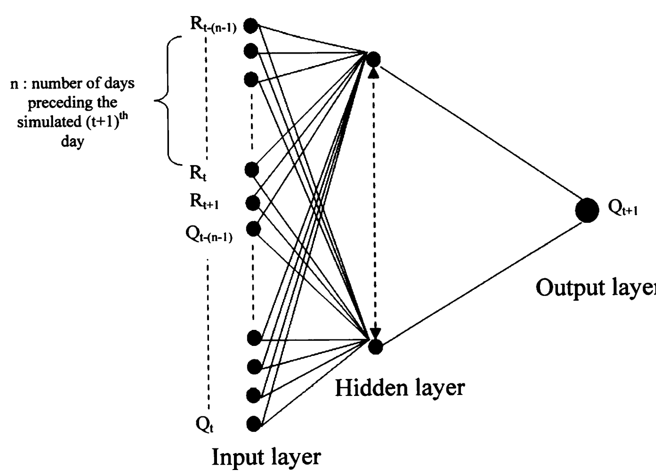

Fig. 5 General architecture of the ANN used to simulate rainfall-discharges relationships of the La Rochefoucauld karst. *R* daily rainfall (mm); *Q* discharges (m^3/s); *n*: number of days preceding the day on which discharge is simulated

 DOI 10.1007/s10040-006-0077-5

Table 1 Data splitting for the three phases of the ANN operation

ANN phase	Beginning	End	Number of days
Training	01/01/1980	31/12/1982	1,096
Validation	01/01/1983	31/12/1985	1,096
Prediction	01/01/1986	31/12/1986	365

Neural network architecture and specification of the input vector

The artificial neural network used to simulate the La Rochefoucauld karst aquifer has the following characteristics (Fig. 5):

– ANN = three-layer feedforward perceptron (i.e. a MLP)
– Hidden layer = single
– Type of training = back-propagation algorithm
– Optimization algorithm = Levenberg-Marquardt algorithm
– Type of transfer function = the log sigmoid function

The input vector of the ANN includes daily raw rainfall data (R_j) and daily discharges data (Q_j). For each of the three phases (training, validation, and prediction), the ANN model can be written as follows:

$$Q_{t+1} = \mathrm{ANN}\left(R_{t+1}, R_t, \ldots R_{t-(n-1)}, Q_t, \ldots, Q_{t-(n-1)}\right) \tag{9}$$

where Q_{t+1} is the discharge value to be simulated at day t+1; R_j is the daily raw rainfall of the jth day; Q_j is the daily discharge of the jth day; n is the number of days preceding the day t+1, taken into account in the input vector (if n=0, the current time step discharge is simulated vs. the current time step rainfall; if n=1, the current time step discharge is simulated vs. the current time step rainfall and the preceding time step discharge and rainfall; etc.). The variable n is sometimes referred to as the lag of the neural network. This formulation of the input vector allows current and past time information to be taken into account in the ANN model.

Note that in this work, the raw rainfall was used instead of the effective rainfall or recharge of the aquifer. In unconfined karst aquifers, recharge is a complex process (Bonacci 1987; Bakalowicz 1995, 2005; Jukic and Denic-Jukic 2003) and depends on a great number of parameters: effective rainfall; evapotranspiration; faults and fractures networks and their characteristics; karst surface features; karst vertical structure. These parameters are not easily measurable and their use in the input vector of the ANN model may contribute to uncertainty.

The use of the raw rainfall relies on measured data, without any transformation, or any formulation of assumption. In this work, the essential characteristics of the input vector are to be simple and to be represented by only one measurable variable. Consequently, this work differs from other ANN modeling approaches to aquifers, in which the input vector consists of a substantial number of variables. Lallahem and Mania (2003) used an input vector including six variables (effective rainfall, mean temperature, potential evapotranspiration, water level, crack flow, infiltration).

Data normalization

The output of the sigmoid transfer function lies in the interval (0, 1). For this reason, the original data are linearly transformed into the interval (0.1, 0.9) before being introduced into the network. The interval (0.1, 0.9) is chosen instead of interval (0, 1) because the sigmoid transfer function is an asymptotic function, so it never reaches the value of 0 nor 1. Thus rainfall and discharge

Fig. 6 Variation of the determination coefficient R^2 according to n (number of days preceding the simulated day)

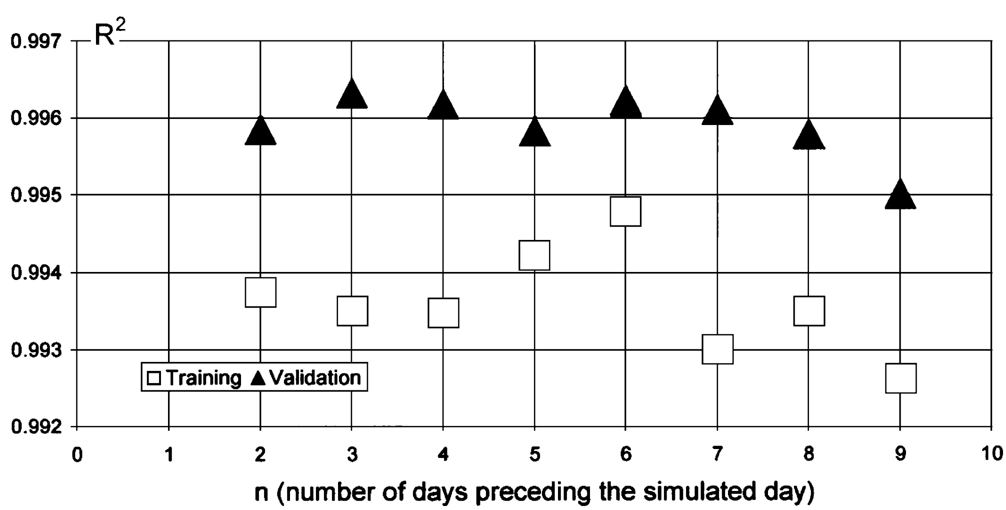

 DOI 10.1007/s10040-006-0077-5

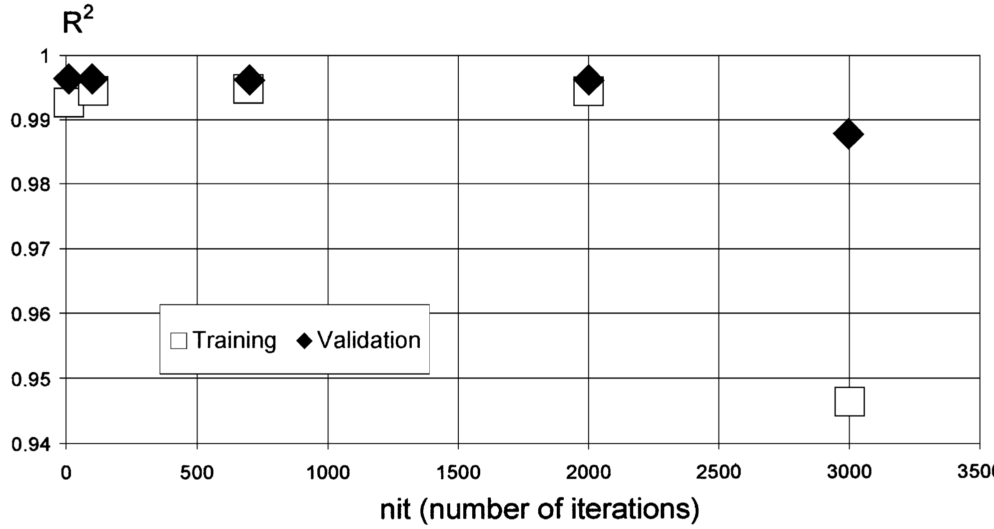

Fig. 7 Variation of the determination coefficient R^2 according to *nit* (number of iterations)

data are preprocessed before being dealt with by the ANN. Preprocessing is done using the following equations:

$$\overline{\overline{R}}_{\mathrm{j}} = 0.1 + 0.8\left(R_{\mathrm{j}}/R_{\max}\right) \tag{10}$$

$$\overline{\overline{Q}}_{\mathrm{j}} = 0.1 + 0.8\left(Q_{\mathrm{j}}\Big/Q_{\max}\right) \tag{11}$$

Once the modeling task is achieved, all transformed data are back-transformed as follows:

$$R_{\mathrm{j}} = \left[\left(\overline{\overline{R}}_{\mathrm{j}} - 0.1\right) \times R_{\max}\right]\Big/0.8 \tag{12}$$

$$Q_{\mathrm{j}} = \left[\left(\overline{\overline{Q}}_{\mathrm{j}} - 0.1\right) \times Q_{\max}\right]\Big/0.8 \tag{13}$$

Data splitting

For the training, validation and prediction phases, the data collected over 7 years were split up in three sets as shown in Table 1. As the training of the ANN is the most crucial phase, the data collected over the first 3 years were assigned to the training phase and the data collected over the three following years were assigned to the validation phase. The data collected over the last year were used to test the prediction ability of the calibrated ANN.

Preliminary tests, training and validation of the ANN model

Several preliminary tests were carried out in order to determine basic parameters needed for the ANN operation. Only the training and validation phases were considered for these tests. The first test relates to the

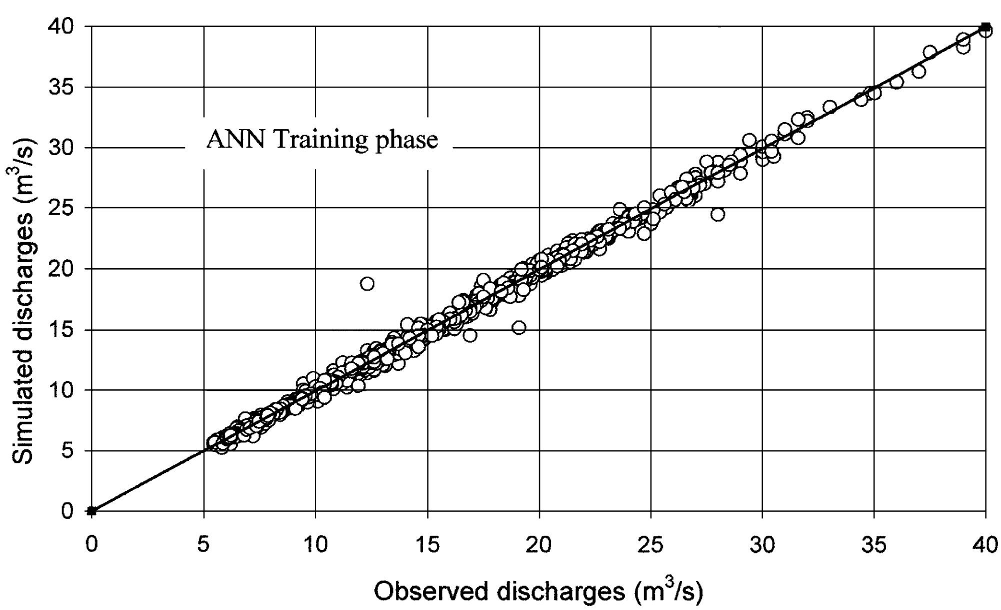

Fig. 8 Scatter plot of simulated discharges vs. observed discharges for the training phase of the ANN

DOI 10.1007/s10040-006-0077-5

number of preceding days (n) that should be considered in Eq. (9). The most recent rainfall time period that actually influences the karstic system discharge of a given day must be specified. The second test relates to the optimum number of iterations needed to perform the optimization procedure. Along with these two tests, the right number of neurons in the hidden layer was also searched for.

Most of the ANN runs were completed by modifying these three parameters according to a trial-and-error procedure. The number n of preceding days was tested between 2 and 9. The number of iterations was tested between 10 and 3,000. The first noticeable result of these tests is that the ANN model converges well for a number of 15 neurons in the hidden layer. This figure was kept during all the other runs.

Figure 6 shows the variation of the determination coefficient R^2 according to the number n of preceding days. The number of hidden neurons is 15 and the number of iterations was fixed to 700 (see the next section Prediction of the karst daily discharges vs. daily raw rainfall: results and discussion). The graph indicates that R^2 remains higher than 0.99, whatever the value of n between 2 and 9. A detailed analysis shows than n=6 is a very satisfactory compromise. Indeed, for this value of n, R^2 has the highest value for the training phase and is quite high for the validation phase.

Results regarding the number of iterations (nit) are reported in Fig. 7. The number of hidden neurons is still 15 and the number of preceding days is 6. The results show that R^2 slightly increases when the number of iterations (nit) increases up to nit=2,000. A number of iterations of 700 is a very satisfactory compromise. It should be noted that increasing nit beyond 2,000 is useless since R^2 falls dramatically (especially for the training phase).

Performance of the ANN model, on the basis of these parameters, is shown in Fig. 8 (training phase) and Fig. 9 (validation phase). Figures 8 and 9 illustrate a very good agreement between the observed daily discharges and those simulated by the ANN model. The ANN model can thus be considered as well calibrated.

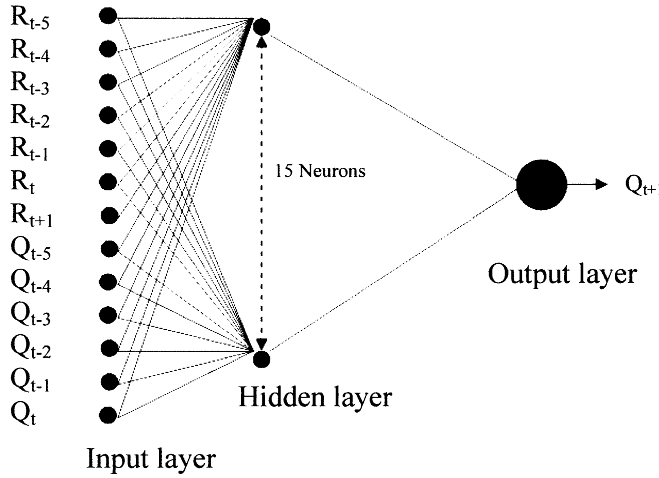

Fig. 10 Actual architecture of the ANN used for the prediction phase

Prediction of the karst daily discharges vs. daily raw rainfall: results and discussion

The previous tests made it possible to set the number of iterations at 700, the number of preceding days at 6, the number of hidden neurons at 15, and to train the ANN. On the basis of these parameters and using the trained ANN, the ability of the ANN to predict the daily discharges of the La Rochefoucauld karst was investigated. The architecture of the ANN model is reported in Fig. 10. The input vector includes 13 elements, among which 7 are daily raw

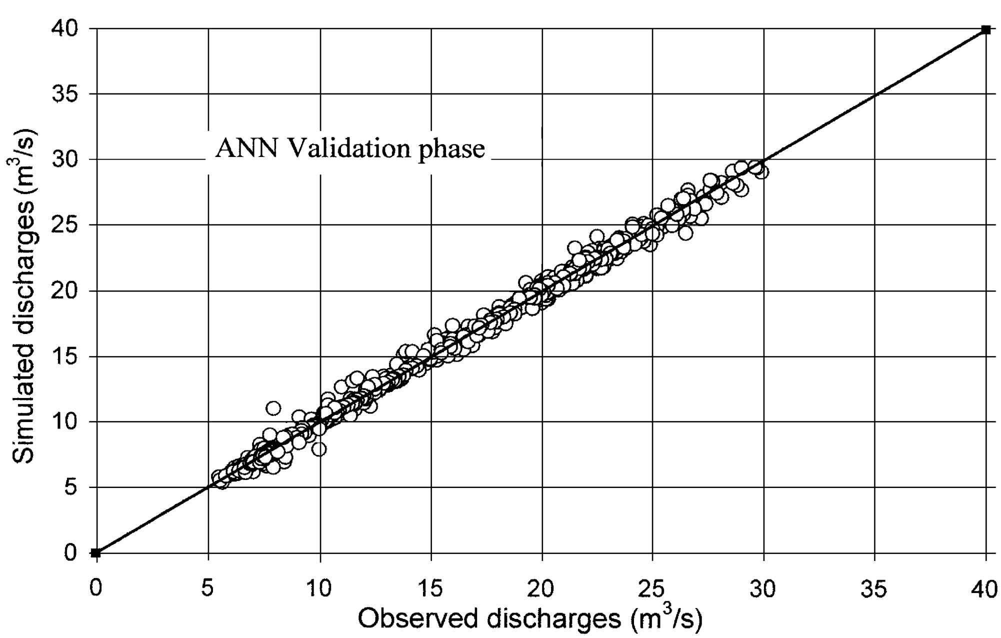

Fig. 9 Scatter plot of simulated discharges vs. observed discharges for the validation phase of the ANN

 DOI 10.1007/s10040-006-0077-5

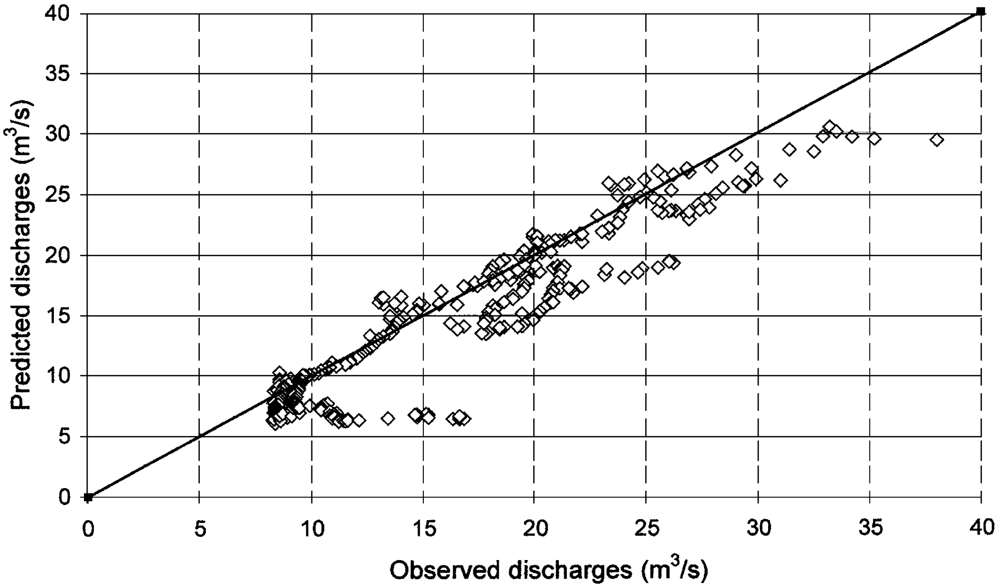

Fig. 11 Correlation diagram between predicted daily discharges vs. observed daily discharges

rainfall values and 6 are daily discharge values. The ANN model can be written as follows:

$$Q_{t+1} = \mathrm{ANN}(R_{t+1}, R_t, R_{t-1}, R_{t-2}, R_{t-3}, R_{t-4}, R_{t-5}, Q_t, Q_{t-1}, Q_{t-2}, Q_{t-3}, Q_{t-4}, Q_{t-5}) \quad (14)$$

On the first day, modeling started with six known discharge values. Subsequently, each predicted daily discharge was used in the input array. From day 7, discharge values introduced as inputs were solely those predicted the six previous days. Results of the ANN model simulation of the La Rochefoucauld karst daily discharges, from 1 January 1986 to 31 December 1986 (365 days) are reported in Figs. 11, 12 and 13. Summary statistics of the simulated and observed discharge series are reported in Table 2. Statistics for the residual errors are given in Table 3.

Figure 11 shows the correlation diagram of the predicted daily discharges vs. the observed daily discharges. Figure 12 shows the predicted daily discharges and the corresponding raw daily rainfall. Figure 13 compares the predicted and observed hygrographs.

Table 2 indicates that the summary statistics of both series (observed and predicted daily discharges) are comparable. The average values are of the same magnitude and the standard deviation values are equivalent. The coefficients of variation show that the dispersion about the average value is almost identical. However, the maximum value of the simulated series is lower than the observed maximum value. The correlation diagram (Fig. 11) shows that most of the points are plotted close to the line y=x. A

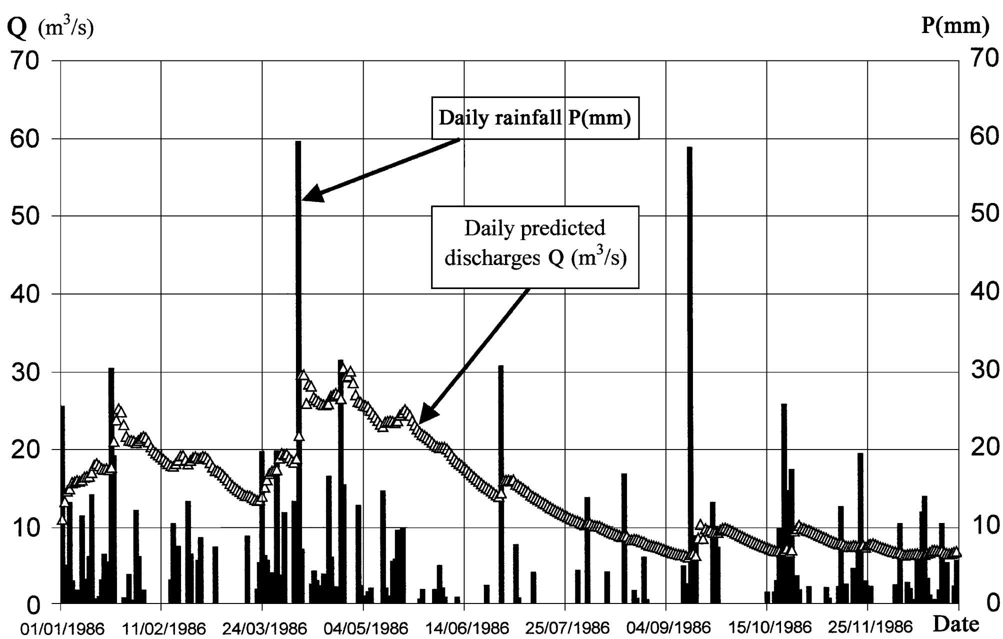

Fig. 12 Predicted daily discharges and the corresponding raw daily rainfall

DOI 10.1007/s10040-006-0077-5

Fig. 13 Predicted and observed hygrographs of the karst aquifer

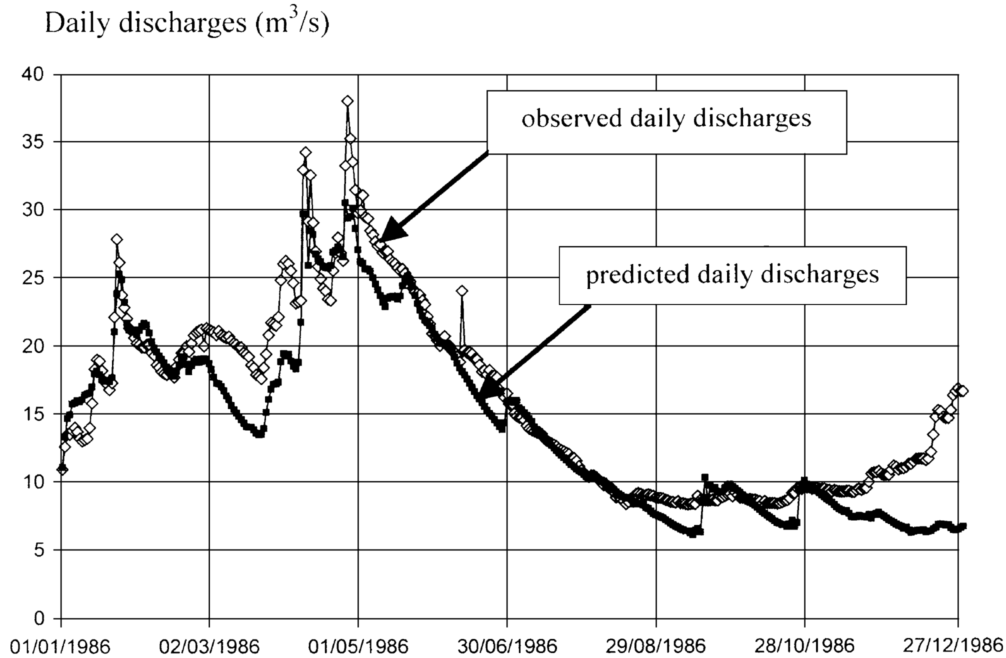

few points, including high and low discharge values, deviate from this line, suggesting that the ANN model does not simulate correctly these extreme values. This relative inability of the ANN to accurately predict extreme discharges is examined using the cumulative distribution functions of the three data sets used for the training, validation and prediction phases (Fig. 14). It is mentioned in the literature (Flood and Kartam 1994; Minns and Hall 1996; Maier and Dandy 2000) that ANNs are typically ineffective in extrapolating beyond the range of the data used for training. According to Heuvelman et al. (2006), both learning and validation data sets should be similar and contain a representative set of high and low values. Comparing the three distribution diagrams (Fig. 14) shows that the training data set includes all the prediction data, but the validation data set does not. The ANN thus does not attempt to extrapolate beyond the range of the training data, but the data sets used for training and validation are different. This could explain the relative inefficiency of the ANN model to predict the extreme discharge values. This issue however requires further investigation, and will require training and validation of the ANN on larger data sets (of the order of a decade).

Table 3 shows the statistics of the residuals errors. The mean error is rather small and negative (ME=−1.6 m^3/s), indicating that the ANN model, on average, slightly underpredicts the discharges. The mean absolute error (MAE) is 2.1 m^3/s and the root mean square error (RMSE) is 2.9 m^3/s. These criteria indicate the size of the prediction error though the RMSE assumes that larger prediction errors are of greater importance than smaller ones. Values for both criteria are, however, quite moderate. The determination coefficient is high (R^2=0.86), indicating that the overall prediction of the daily discharges is acceptable, even satisfactory. Figure 12 displays the series of predicted discharges and the series of corresponding raw rainfall. Note that the rising parts of the predicted hydrograph correspond quite well with heavy rainfall. The time lag between rainfall and discharges corresponds to a few days. Similarly, the recession parts correspond with periods of low rainfall (or no rainfall). Consequently, the ANN model properly accounts for the operational specificities of a karst aquifer. A comparison between observed and predicted hydrographs (Fig. 13) shows that the overall shapes of both hydrographs are consistent.

These findings suggest that the trained ANN model is fully operational for predicting the La Rochefoucauld karst aquifer daily discharges using the raw daily rainfall.

Table 2 Summary statistics of the observed (Q_{obs}, m^3/s) and predicted (Q_{pred}, m^3/s) daily discharge series of the La Rochefoucauld karst aquifer

	Min (m^3/s)	Max (m^3/s)	Average (m^3/s)	SD (m^3/s)	CV (%)
Q_{obs}	8.3	38.0	15.9	6.7	42
Q_{pred}	6.0	30.5	14.3	6.6	46

Min minimum value; *Max* maximum value; *SD* standard deviation; *CV* coefficient of variation

Table 3 Statistics of the residual errors between the observed (Q_{obs}) and predicted (Q_{pred}) daily discharge series (in m^3/s)

ME (m^3/s)	MAE (m^3/s)	RMSE (m^3/s)
−1.6	2.1	2.9

ME mean error; *MAE* mean absolute error; *RMSE* root mean square error

 DOI 10.1007/s10040-006-0077-5

Conversion of raw rainfall data into effective rainfall data or recharge is not necessary. This represents an unquestionable advantage, since assumptions on the transformation of raw rainfall into effective rainfall are no longer needed.

Conclusions and perspectives

This paper focuses on the evaluation of the ability of the artificial neural networks (ANN) to simulate input–output responses of karst aquifers. Karst aquifers are recognized

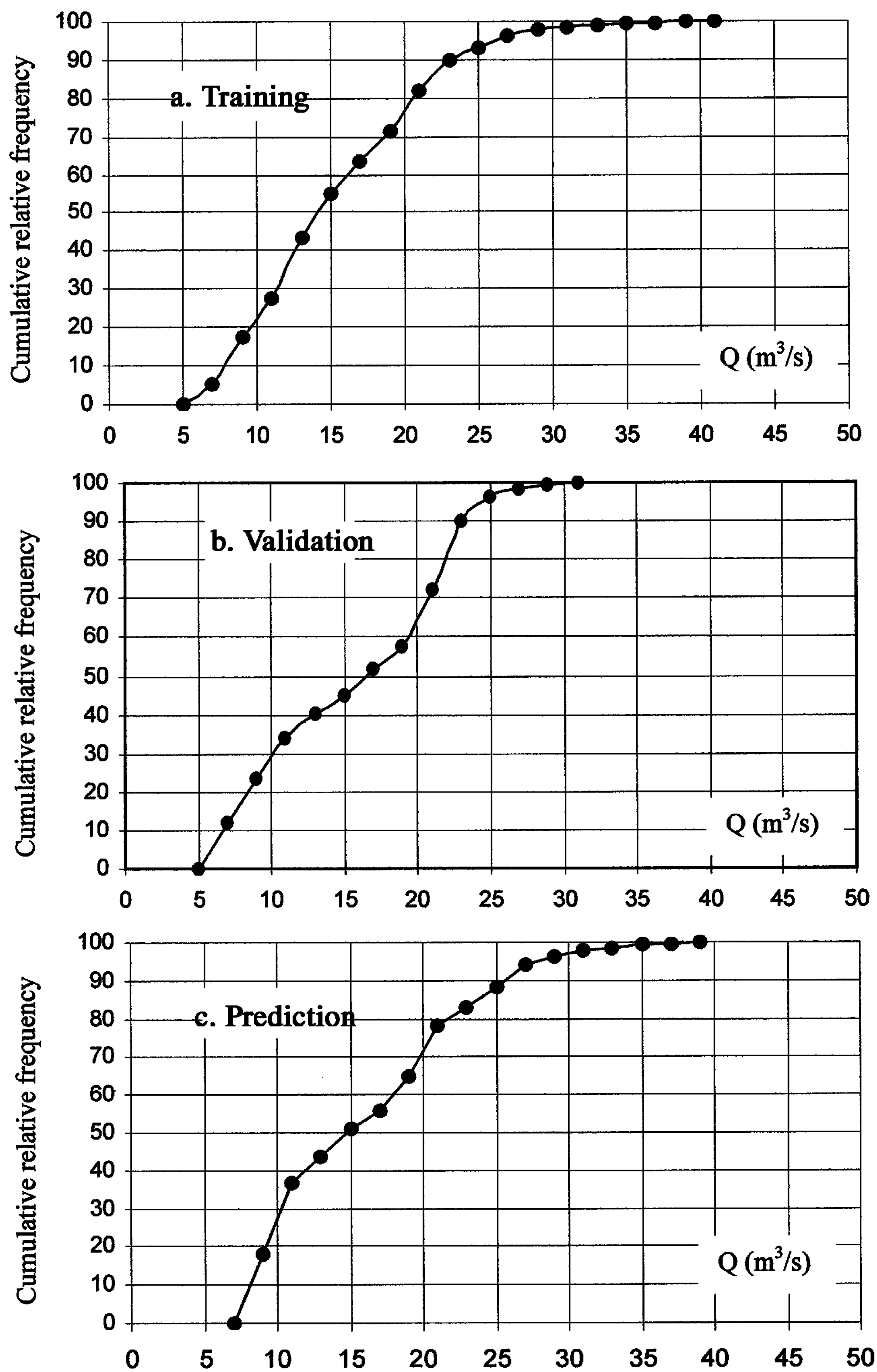

Fig. 14 Cumulative distribution functions of the data sets used for the **a** training, **b** validation and **c** prediction phases of the ANN

DOI 10.1007/s10040-006-0077-5

in the hydrogeology literature (White 1969; Mangin 1984; Labat et al. 2002) as complex non-linear and hierarchical systems. They contain significant water resources and, accordingly, they should be properly managed using modern tools such as numerical models. Distributed numerical models proved successful in simulating karst aquifers on a regional scale but are limited by the need for large databases. Thereafter, the applicability of the ANN methodology is tested taking into account the raw daily rainfall only as input of the model to simulate the karst aquifer daily discharges.

The main points associated with this work are listed below:

1. An ANN model has been developed to simulate the daily raw rainfall–daily discharge relationships in a large karst aquifer (the La Rochefoucauld karst aquifer, south-western France). The daily data used here span seven years. Three years are assigned to the training phase of the ANN, 3 years to the validation phase and 1 year to the testing of the ANN predictive ability.
2. The ANN structure is a three-layer feed forward network including one input layer, one hidden layer and one output layer. The training of the ANN is performed using the back-propagation Levenberg-Marquardt algorithm.
3. The preliminary tests allow determination of the optimum temporal information to be included in the input data to simulate the ith day discharge: the number of days preceding the ith day is 6.
4. The training and validation phases led to a very satisfactory calibration of the neural network. The determination coefficient of simulated vs. observed daily discharges is, for both phases, higher than 0.99. The ANN approach captures well the most important features of the karst system dynamics.
5. The prediction phase shows that simulated daily discharges are statistically comparable to observed discharges. The ANN model operates like a karst system. Rising parts of the simulated hydrograph are abrupt and correspond well to heavy rainfall periods, whereas the recession parts correspond to periods with low (or no) rainfall. The overall shape of the predicted hydrograph is equivalent to that of the observed hydrograph.

Note that in usual hydrogeological modeling procedure, raw rainfall is first transformed into effective rainfall (i.e. recharge), which requires some uncontrolled assumptions and thus might introduce uncertainty in the procedure. In this work, the use of raw rainfall avoids such assumptions and simplifies the modeling procedure. This constitutes a key advantage of the ANN method as used here. In addition, the ANN model provides other non-negligible advantages because no data about the karst internal structure (transmissivity, storage coefficient, geometry, ...) are needed.

These results are undoubtedly encouraging as the trained neural network is capable of operating like karst aquifers with all their specificities. The ANN methodology does show potential for the modeling of karst aquifers, taking into account all their specificities, and offers novel prospects in this field.

However, further research is needed since the highest daily discharges were not reproduced by the ANN in the present work. Thus in forthcoming works, the following tracks will be investigated:

- A more thorough training of the network over much longer periods (of the order of one decade).
- Introduction of additional variables (piezometry; evapotranspiration, etc.) into the network input vector. However, one should keep in mind that the ANN model as built here is simple and robust, for it uses one single variable as input (raw daily rainfall), which in the authors' opinion, is a major advantage. Additional variables might require additional assumptions and consequently reduce the simplicity and robustness of the ANN model.
- Other types of neural network structures and/or other training algorithms will be tested.

Acknowledgements The authors wish to thank the managing editor, Prof. Maria-Theresia Schafmeister, the associate editor, reviewer Dr. Richard Preston and two anonymous reviewers for their helpful comments, which contributed much to the improvement of this paper.

References

Amraoui F, Razack M, Bouchaou L (2003) Turbidity dynamics in karstic systems: example of Ribaa and Bittit springs in the Middle Atlas (Morocco). Hydrol Sci J 48(6):971–984
Angelini P, Dragoni W (1997) The problem of modeling limestone spring: the case of Bagnara (North Apennines, Italy). Ground Water 35(4)612–618
Aziz AR, Wong KFV (1992) A neural network approach to the determination of aquifer parameters. Ground Water 30(2): 164–166
Bakalowicz M (1995) La zone d'infiltration des aquifères karstiques: méthodes d'étude, structure et fonctionnement (The infiltration zone of karstic aquifers: study methods, structure and functioning). Hydrogéologie 4:3–21
Bakalowicz M (2005) Karst groundwater: a challenge for new resources. Hydrogeol J 13:148–160
Balkhair KS (2002) Aquifer parameters determination for large diameter wells using neural network approach. J Hydrol 265:118–128
Barrett J, Charbeneau RJ (1996) A parsimonious model for simulation of flow and transport in a karst aquifer. Center for Research in Water Resources, University of Texas, Austin, Technical Rep. 269 http://www.crwr.utexas.edu. Cited March 2006
Beale R, Jackson T (1991) Neural computing: an introduction. Techno House, Bristol, UK
Bonacci O (1987) Karst Hydrology. Springer-Verlag, Berlin Heidelberg New York
Cheng B, Titterington DM (1994) Neural networks: a review from a statistical perspective. Statist Sci 9(1)2–54
Demuth H, Beale M (2003) 'Neural networks toolbox' user guide. Mathworks Inc., Natick, MA
Drogue C (1992) Hydrodynamics of karstic aquifers: experimental sites in the Mediterranean karsts, southern France. In: Back W, Herman JS, Paloc H (eds) Hydrogeology of selected Karst Regions. Int Contrib Hydrogeol 13:133–149

Fausett L (1994) Fundamentals of neural networks: architecture, algorithms and application. Prentice Hall, Englewood Cliffs, NJ
Flood I, Kartam N (1994) Neural networks in civil engineering: principles and understanding. J Comput Civ Eng 8(2):131–148
Ford DC, William PW (1989) Karst geomorphology and hydrology. Unwin Hyman, London
French M, Krajewski W, Cuykendall R (1992) Rainfall forecasting in space and time using a neural network. J Hydrol 137:1–31
Hagan MT, Menhaj MB (1994) Training feedforward networks with the Marquardt algorithm. IEEE Trans Neural Netw 5:989–993
Hagan MT, Demuth HB, Beale MH (1996) Neural network design. PWS, Boston, MA
Halff AH, Halff HM, Azmoodeh M (1993) Predicting runoff from rainfall using neural networks. Proc Eng Hydrol, ASCE, New York, pp 768–775
Heuvelman G, Muys B, Feyen J (2006) Regionalisation of the parameters of a hydrological model: comparison of linear regression models with artificial neural nets. J Hydrol 319:245–265
Hsu K, Gupta HV, Sorooshian S (1995) Artificial neural network modeling of the rainfall-runoff process. Wat Resour Res 31 (10):2517–2530
Huntoon PW (1995) Is it appropriate to apply porous media groundwater circulation models to karstic aquifers? In: El-Kadi AI (ed) Groundwater models for resources analysis and management, Pacific Northwest/Oceania Conf., Honolulu, HI, CRC Press, Boca Raton, FL, pp 339–358
Imrie CE, Durucan S, Korre A (2000) River flow prediction using artificial neural networks: generalization beyond the calibration range. J Hydrol 233:138–153
Jukic D, Denic-Jukic V (2003) A frequency domain approach to groundwater recharge estimation in karst. J Hydrol 289:95–110
Kiraly L (1975) Rapport sur l'état actuel des connaissances dans le domaine des caractères physiques des roches karstiques (Report on the present state of knowledge about the physical characteristics of karstic rocks). In: Burger A, Dubertret L (eds) Hydrogeology of karstic terrains. Int Union Geol Sci Ser B 3:53–67
Kruseman G, de Ridder NA (1994) Analysis and evaluation of pumping tests data. Bull. No. 47, International Institute for Land Reclamation and Improvement, Wageningen, The Netherlands, p 377
Kuo YM, Liu CW, Lin KH (2004) Evaluation of the ability of an artificial neural network model to assess the variation of groundwater quality in an area of blackfoot disease in Taiwan. Water Res 38:148–158
Labat D, Ababou R, Mangin A (2002) Analyse multirésolution croisée de pluie et débits de sources karstiques (Multi-resolution cross analysis of rainfall rates and karstic springs runoffs). C R Geoscience 334(8):51–556
Lallahem S, Mania J (2003) A non-linear rainfall-runoff model using neural network technique: example in fractured porous media. Math Comput Model 37:1047–1061
Larocque M, Razack M (1998) Synthèse hydrogéologique de l'aquifère de La Rochefoucauld: bilan des nouvelles connaissances (Hydrogeological synthesis of La Rochefoucauld karst aquifer: review of new data). Hydrogéologie 3:35–45
Larocque M, Banton O, Ackerer P, Razack M (1999) Determining karst transmissivities with inverse modeling and an equivalent porous media. Ground Water 37:897–903
Maier HR, Dandy GC (2000) Neural networks for the prediction and forecasting of water resources variables: a review of modelling issues and applications. Environ Model Softw 15:101–124
Mangin A (1984) Pour une meilleure connaissance des systèmes hydrologiques à partir des analyses corrélatoires et spectrales (Towards a better knowledge of hydrologic systems using correlation and spectral analysis). J Hydrol 67:25–43
Maren AJ (1990) Neural networks structures. In: Maren AJ, Harston CT, Pap RM (eds) Handbook of neural computing and applications. Academic Press, San Diego, CA
Maren AJ, Harston CT, Pap RM (1990) Handbook of neural computing applications. Academic Press, San Diego, CA 92101
Masters T (1993) Practical neural networks. Academic Press, San Diego, CA
Medsker L (1994) Hybrid neural network and expert systems. Kluwer Academic, Boston, MA
Minns AW, Hall MJ (1996) Artificial neural networks as rainfall-runoff models. Hydrol Sci J 41(3):399–417
Moré JJ (1978) The Levenberg-Marquardt algorithm: implementation and theory. In: Watson GA (ed) Lecture notes in mathematics 630. Springer, Berlin Heidelberg New York, pp 5–116
Morshed J, Kaluarachchi JJ (1998) Application of artificial neural networks and genetic algorithm in flow and transport simulation. Adv Water Resour 22(2):145–158
Padilla A, Pulido-Bosch A (1995) Study of hydrographs of karstic aquifers by means of correlation and cross-spectral analysis. J Hydrol 168:73–89
Press WH, Teukolski SA, Vetterling WT, Flannery BP (1992) Numerical recipes in Fortran, 2nd edn. Cambridge Univ. Press, New York, pp 675–683
Quélennec R, Sauret JC, Séguin M, Vouvé J (1971) Les résurgences de la Touvre: etude préliminaire (The spring of La Touvre: preliminary study). Proc Int. Symp. Hydrologie en pays calcaires, Univ. Besançon, France, pp 197–205
Rahnemai M, Zare M, Nematollahi AR, Sedghi H (2005) Application of spectral analysis of daily water level and spring discharge hydrographs data for comparing physical characteristics of karstic aquifers. J Hydrol 311:106–116
Rajurkar MP, Kothyari UC, Chaube UC (2004) Modeling of the daily rainfall-runoff relationship with artificial neural network. J Hydrol 285:96–113
Rambaud D (1979) Hydrogéologie du Département de la Charente. Principaux systèmes aquifères: essai d'analyse et cartographie (Hydrogeology of the Department of Charente. Principal aquifer systems: analysis and cartography). PhD Thesis, Bordeaux III University, France
Ranjithan SJ, Eheart JW, Garett JH (1993) Neural network based screening for groundwater reclamation under uncertainty. Water Resour Res 29(3):563–574
Rogers LL, Dowla FU, Johnson VM (1995) Optimal field scale groundwater remediation using neural networks and the genetic algorithm. Env Sci Tech 29(5):1145–1155
Ross JH, Rieg A, Leibundgut C (2001) Tracer study on the tectonic control of the drainage system in the contact karst zone of Lake Voralp (Swiss Alps). Acta Carsol 30/2(15):203–213
Rouiller D (1987) Etude des systèmes karstiques de la Touvre et de la Lèche (Angoulême, Charente) (Study of the karstic systems of La Touvre and of La Lèche, Angouleme, Charente). PhD Thesis, University of Avignon, France
Sajikumar N, Thandaveswara BS (1999) A nonlinear rainfall runoff model using an artificial neural network. J Hydrol 216:32–55
Scanlon BR, Mace RE, Barrett ME, Smith B (2003) Can we simulate regional groundwater flow in a karst system using equivalent porous media models? Case study, Barton Springs, Edwards aquifer, USA. J Hydrol 276:137–158
Shamseldin AY (1997) Application of a neural technique to rainfall-runoff modelling. J Hydrol 199:272–294
White WB (1969) Conceptual model for carbonate aquifers. Ground Water 7:15–21
Zio E (1997) Approaching the inverse problem of parameter estimation in groundwater models by means of artificial neural networks. Prog Nucl Energy 31:303–315

 DOI 10.1007/s10040-006-0077-5